NUCL SCI TECH (2019) 30:169
https://doi.org/10.1007/s41365-019-0684-1

A possible scheme for the surface muon beamline at CSNS

Lu-Ping Zhou[1,2,3] · Qi-Li Mu[2,3,5] · Han-Tao Jing[2,3] · Jing-Yu Tang[1,2,3] · Yu Bao[2,3] · Ying-Peng Song[2,3,4]

Received: 30 January 2019 / Revised: 13 May 2019 / Accepted: 14 May 2019 / Published online: 24 October 2019

Abstract An experimental muon source is planned for the China Spallation Neutron Source. A simplified beamline with a limited number of magnets is achieved using a FODO lattice for implementation in a future preliminary stage. The yield of the muon delivered to the experimental sample is slightly larger than 10^5 μ^+/s within the FWHM beam spot ($\sim$ Ø30 mm) from a thick muon target. In addition, the beam polarization is 92% and the contamination that is mainly formed by positrons is approximately a fraction of 1%.

Keywords CSNS · Polarized muon beamline · Carbon target · FODO lattice

This work was supported by the National Natural Science Foundation of China (Nos. 11575217, 11527811).

✉ Lu-Ping Zhou
zhoulp@ihep.ac.cn

Qi-Li Mu
muql@ihep.ac.cn

[1] University of Chinese Academy of Sciences, Beijing 100049, China

[2] Institute of High Energy Physics, Chinese Academy of Sciences, Beijing 100049, China

[3] Spallation Neutron Source Science Center, Dongguan 523803, China

[4] University of Science and Technology of China, Hefei 230026, China

[5] Jilin University, Changchun 130012, China

1 Introduction

Today, there are four muon sources for μSR experiments and other applications. SμS [1, 2] at PSI has the most intense quasi-continuous muon beam source in the world and includes a total of five beamlines. Due to the megawatt power of the proton beam and the moderate thickness of the target, the surface muon flux of the large-aperture μE4 beamline [3] can reach a magnitude of 10^8 μ^+/s. This beamline is an injector for the only slow-muon beamline (LEM now) in the world. At TRIUMF-CMMS, there is also a continuous proton beam to drive a muon source consisting of four muon beamlines [4, 5]. The M13 and M15 lines are mainly designed for surface muons. The muon sources at J-PARC and ISIS are pulsed muon sources. The ISIS muon source includes three terminals: Emu, MuSR, and HiFi [6]. The RIKEN-RAL muon beamline can deliver both surface muon and decay muon beams with momenta up to 100 MeV/*c* [7]. At J-PARC [8–10], the D-line can deliver decay or surface muons to experimental terminals. Commissioned in 2017, the S-line is a new surface muon beamline dedicated to experiments on condensed matter physics. Some parameters of surface muon beamlines for these four muon sources, as well as EMuS, are given in Table 1.

In 2018, China completed the construction of the China Spallation Neutron Source (CSNS) [11], which provides the condition required to build a muon source. It consists of a 1.6-GeV proton accelerator and a target station for producing neutrons, as shown in Fig. 1. The proton beam bombards a tungsten target with a power of 100 kW at phase I. In the future, the proton beam power will be upgraded to 500 kW. At present, an experimental muon source (EMuS) has been schemed in the high-energy

Table 1 Performance of surface muon beam (including EMuS baby scheme)

	Surface muon beam line	Magnitude of flux (μ^+/s)	Beam spot (mm^2)	Contamination	Momentum distribution
J-PARC, MUCE	D-line, S-line	10^7	30 × 40 ($H \times V$)	–	~ 15%
ISIS muon source	ISIS	10^5–10^6	10–30 × 10 ($H \times V$)	$e^+/\mu^+ < 15\%$	7%, centered at 27 MeV/c
	RIKEN-RAL	10^5–10^6	Ø10–50, adjustable	–	
PSI-SμS	πE3	10^7	15 × 30 ($H \times V$)	e^+/μ^+: 1–2%	8%, centered at 28 MeV/c
	μE4	10^8	25 × 35 ($H \times V$), WSX-off	e^+/μ^+: 1%	1.8–11%
TRIUMF-CMMS	M13	10^5	30 × 20 ($H \times V$)	–	20–30 MeV/c
	M15	10^6	12 × 16 ($H \times V$)	–	19–40 MeV/c
EMuS	Baby scheme	10^5	Ø30	e^+/μ^+ : 1%	~ 10%, centered at 28 MeV/c

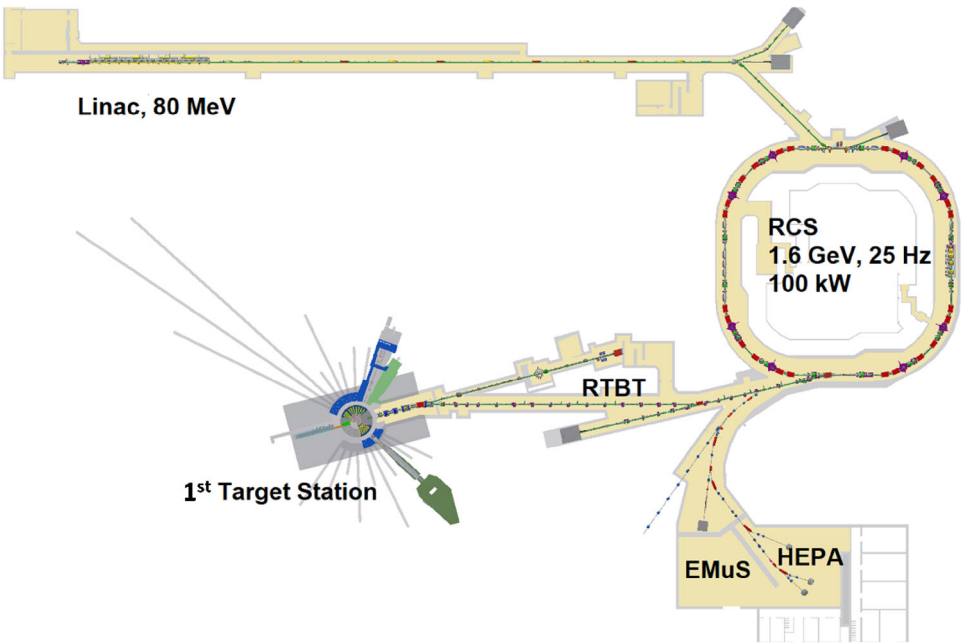

Fig. 1 Layout of CSNS including HEPA

proton experimental area (HPEA) at CSNS [12]. Approximately 5% of the proton beams will be extracted from the ring-to-target beam transport beamline (RTBT) and delivered to the EMuS. Limited by the available budget, a simplified muon source (also referred to as the baby scheme) will be initially built. In this report, a baby scheme beamline based on room-temperature magnets is designed.

2 Surface muons from the target

2.1 Layout of the target area

In general, a high-energy proton beam bombards a carbon target to produce a large number of pions. A pion soon decays to a corresponding charge-state muon and a neutrino. Given that negative pions are mostly captured by target nuclei, the negative muon yield is much lower than that of the positive muon yield. Therefore, the positive muons are used in multi-purpose studies based on the μSR (muon spin resonance, relaxation, and rotation) method. Usually, positive muons are classified into three categories: decay muons, cloud muons, and surface muons. Decay muons are produced from pions that decay in flight. Low-energy pions soon decay to muons in the region of the target and form so-called cloud muons. Surface muons refer to the muons produced from the decay associated with stopping pions near the surface area of the target, as shown in Fig. 2.

Apart from the commonly used graphite target, other materials such as beryllium, copper, and tungsten can also be used to produce pions and muons. For example, the muon sources at KEK and TRIUMF once employed a beryllium target [13]. According to previous research [12], the yield advantage of the high-Z target is not significant,

but the radiation in the vicinity of the target is substantial. In our design, a carbon target is planned with a size of 10 cm × 5 cm × 1.5 cm. A 5-kW proton beam bombards the thick carbon target, and the surviving proton beam is collimated and then delivered to a beam dump. The surface muons will then be collected at 0.6 m from the lateral side. Figure 3 shows the carbon target and geometry of the target area.

2.2 Muon distribution at entrance and parameters

To obtain more realistic initial beam parameters for the beamline design, FLUKA [14] is employed to simulate the particle interactions and transport processes in the target. The muon phase distributions at the lateral side of the target are scored. For surface muon applications, the beamline only needs to transport a muon beam with a narrow momentum spread. This is beneficial in reducing the proportion of cloud muons, which effectively promotes beam polarization. Figure 4 illustrates the initial phase map of the muon with momentum in the range between 26 and 29.8 MeV/c at 0.4 m from the center of the target. The center of the momentum range is 28 MeV/c, while the momentum dispersion is approximately 14%. The surface muon will be collected by the first doublet at 0.6 m from the target.

Similar to the beamlines at PSI and ISIS, a beamline with a large transverse acceptance is expected to generate the most intensive muon flux from the low proton beam power of 5 kW at EMuS. In general, with a muon beamline of physical aperture of approximately 400 mm, the lattice based on room-temperature quadrupoles has an acceptable maximal divergence of approximately 120 mrad. Under this upper limit, phase-space ellipses are selected based on the density distribution of muons in the x–x' or y–y' phase planes. According to the previous research [12], considering an expected muon intensity at the sample, a beam emittance of 5200 (horizontal) × 3000 (vertical) π mm mrad at 0.4 m from the right lateral side of the target would be reasonable as an acceptable muon flux. According to the ellipse emittances and maximal divergence, the Twiss parameters could be calculated using Formula 1 where $\beta\gamma - \alpha^2 = 1$. In Fig. 4, the muon density distribution and emittance ellipses are presented. The Twiss parameters are listed in Table 2.

$$x_{\mathrm{m}} = \sqrt{\epsilon_x \cdot \beta_x} = 52.98\,\mathrm{mm}, \tag{1a}$$

$$x'_{\mathrm{m}} = \sqrt{\epsilon_x \cdot \gamma_x} = 120\,\mathrm{mrad}, \tag{1b}$$

$$y_{\mathrm{m}} = \sqrt{\epsilon_y \cdot \beta_y} = 46.15\,\mathrm{mm}, \tag{1c}$$

$$y'_{\mathrm{m}} = \sqrt{\epsilon_y \cdot \gamma_y} = 120\,\mathrm{mrad}. \tag{1d}$$

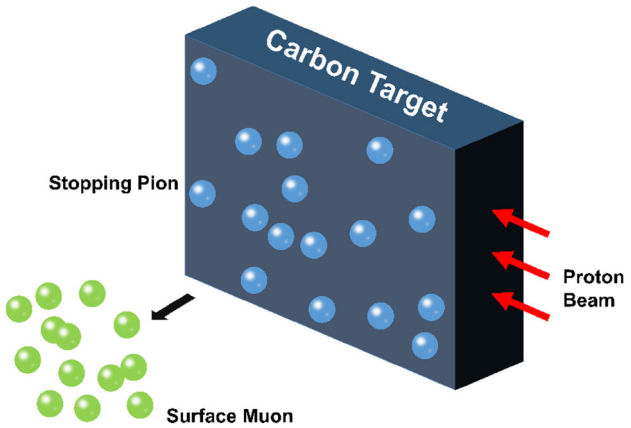

Fig. 2 Surface muons produced from the target

3 Design of surface muon beamline

3.1 Optics and multi-particle simulation

A simplified surface muon beamline with a length of approximately 10 m will facilitate the achievement of several goals with regard to surface muons: (1) collection from the target; (2) transmitting from the target to the experimental terminal; (3) focusing and collimating to a small beam spot; (4) suppression of the in-beam background. Three doublets are used for the collection and transmission of surface muons. Two dipoles are used to obtain a small momentum acceptance and to sweep the neutral particles. A triplet is used to focus the spot focus. A Wien filter is used to sweep out in-beam positrons. The overall lattice structure of the beamline is shown in Fig. 5.

The quadrupoles of the doublets are all at room temperature with an aperture of 400 mm. In addition, the distance between the quadrupoles in a doublet is 0.15 m. Two rectangular bend magnets are used to bend the beam and define the beam momentum spread. Rectangular bend magnets with a deflection angle of 30° are employed. A Wien filter with a short length and strong field strength is placed before the triplet to sweep off in-beam positrons. The specific deflection angle can be calculated using Formula 2a and 2b [3] as follows:

$$\varphi_{\mathrm{E}}\,(\mathrm{mrad}) = l_{\mathrm{E}}(\mathrm{m}) \cdot \frac{E\,(\mathrm{kV/m})}{\beta p\,(\mathrm{MeV}/c)}, \tag{2a}$$

$$\varphi_{\mathrm{B}}(\mathrm{mrad}) = 30 l_{\mathrm{B}}(\mathrm{m}) \cdot \frac{B(\mathrm{G})}{p(\mathrm{MeV}/c)}, \tag{2b}$$

where φ_{E} and φ_{B} are the deflection angles of the magnetic field and electric field, respectively, and l is the length of the field (hard boundary), B and E are the field strength, and p is the momentum of the particles. The units are in

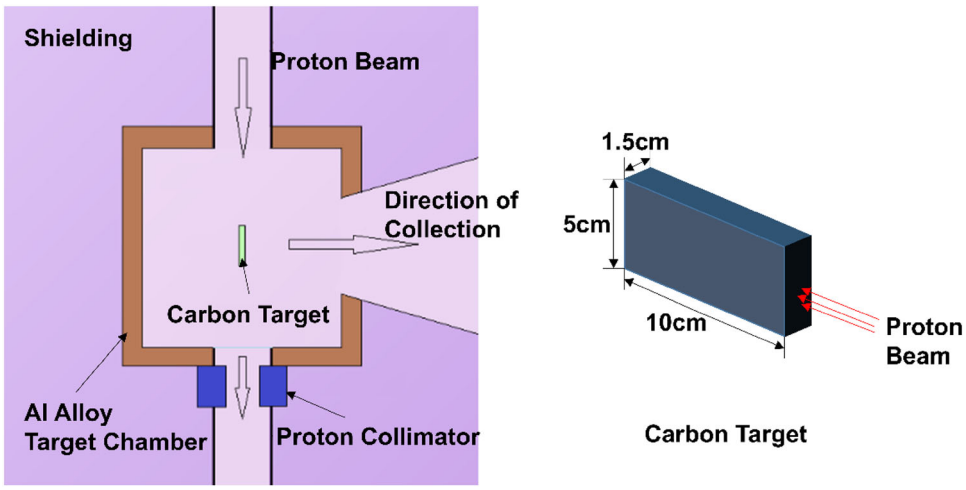

Fig. 3 Target area scheme for the simplified design of EMuS

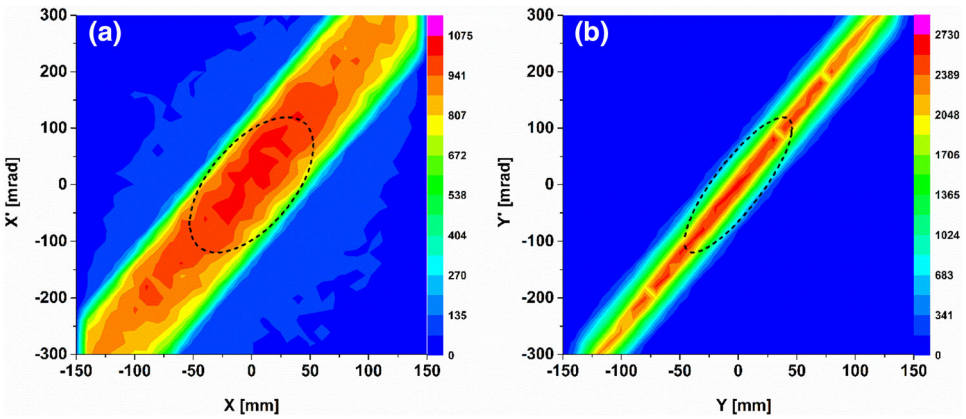

Fig. 4 Initial phase map and emittance ellipses (dashed line) at 0.4 m from the target

Table 2 Initial Twiss parameters (at 0.4 m from target)

Muon momentum (26–29.8 MeV/c)	ϵ_x (π mm mrad)	α_x	β_x (m)	ϵ_y (π mm mrad)	α_y	β_y (m)
	5200	− 0.7	0.54	3000	− 1.55	0.71

parentheses. Apparently, a strong magnetic field with a long length will reduce the beam polarization because it can facilitate both deflection and spin rotation. A compromise between the polarization reduction and positron background level is considered. Based on the initial beamline parameters that were previously mentioned, the optical calculation was started from 0.4 m from the carbon target. Figure 6 shows the horizontal and vertical linear optical envelopes of the beamline using graphic transport [15].

Following the optimal optical design, G4beamline [16] is used to perform the multi-particle simulation for this beamline. In the case of no collimation, the optical parameters are used directly for the multi-particle simulation. The beam spot at the sample position is much larger in the vertical direction than that of the horizontal direction as shown in Fig. 7a, because of nonlinear effects. Hence the triplet is optimally retuned to achieve a better spot in terms of both shape and size. Given that the distribution of the actual surface muons (26–29.8 MeV/c) is almost uniform, a uniform distribution of primary muons is employed in this simulation that is defined by the acceptance phase ellipses, for better statistics in G4beamline. In this case, the transmission efficiency is approximately 88% based on a comparison of the particles in the beam spot with those at the initial position. A total of 12% of the total muons are lost along the beamline, as shown in Fig. 8. More than half of them are lost at the first doublet. The main component parameters of the beamline are given in Table 3.

3.2 Beam collimation

Due to the large emittance of the secondary muon beam and the limitation of the number of components, it is

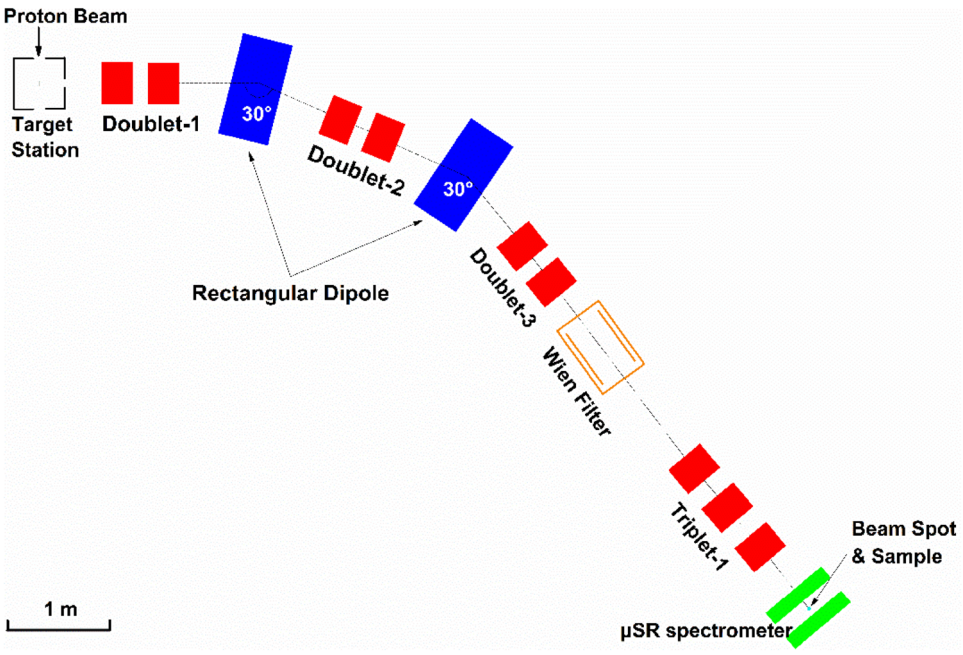

Fig. 5 Layout of the baby scheme muon beamline

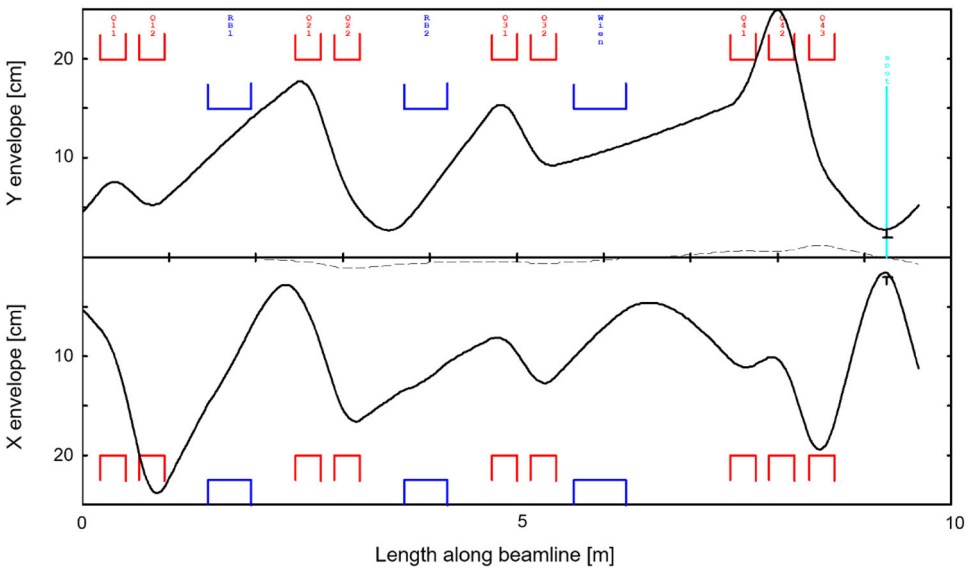

Fig. 6 Linear envelope calculated by TRANSPORT

difficult to implement an adjustable narrow momentum spread and small beam spot for different experiments. In our design, the beam collimation in the beamline is employed to reduce the background and to control the beam spot. Initially, we simulate the nuclear reaction process of proton bombardment on the carbon target by employing FLUKA. All the produced muons, positrons, and other particles are collected before the entrance of beamline and then transported in the lattice of the beamline as a primary beam.

3.2.1 Momentum collimation

Surface muons emitted from the target have the same momentum of approximately 29.8 MeV/*c* if they are not moderated. To obtain higher polarization of the muon beam, it is important to minimize the decay or cloud muons. Given that muons with momentum larger than 29.8 MeV/*c* must be cloud muons, we employ a momentum collimator to intercept them. The normalized dispersion function is considered to identify the suitable positions for momentum collimation,

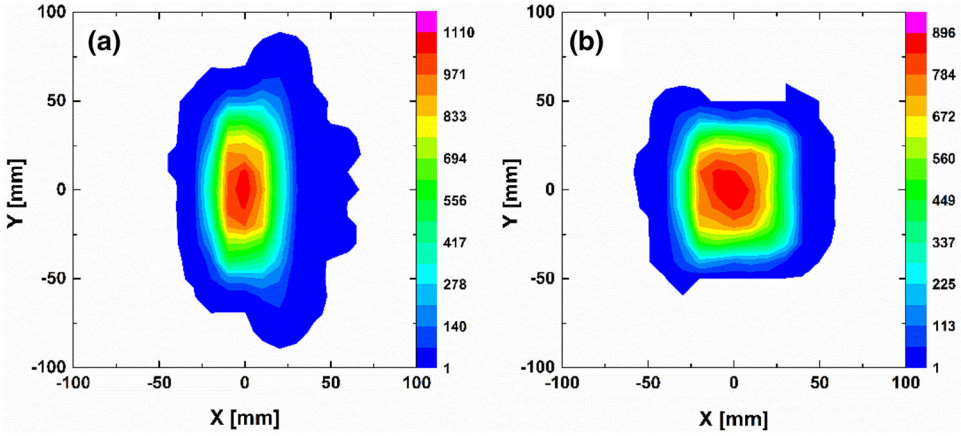

Fig. 7 **a** Graph of beam spot when using the triplet given by TRANSPORT, **b** graph of beam spot when using a retuned triplet

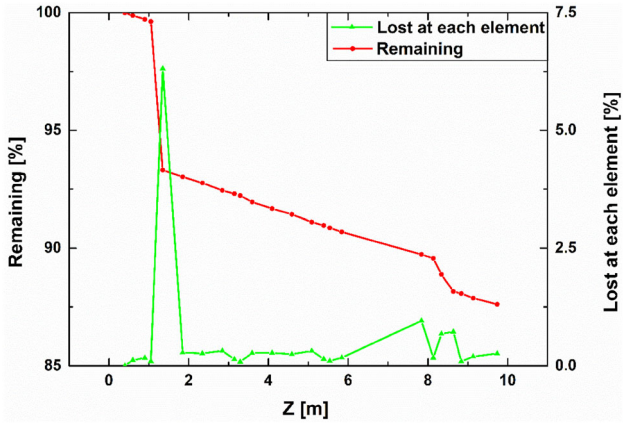

Fig. 8 Beam loss and remaining along the transport line

$$D_{\mathrm{d}} = \frac{D_x}{\sqrt{\beta_x}}, \tag{3a}$$

$$D'_{\mathrm{d}} = \frac{\alpha_x D_x + \beta_x D'_x}{\sqrt{\beta_x}}, \tag{3b}$$

where D_{d} is the horizontal normalized dispersion function, α and β are the Twiss parameters, and D_x is the horizontal dispersion function.

The normalized dispersion function along the beamline is shown in Fig. 9a. After the first dipole, there is a maximum value which is the best collimating position. The μ^+ with momentum larger than 29.8 MeV/c must be cloud muon and will lead to a decrease in polarization. At this position, a portion of the cloud muons can be removed using a collimator placed at approximately x = 70 mm as shown in Fig. 9b. In this case, there are still approximately 10% of the cloud muons remaining in the beam. Considering the requirements of the μSR experiments, an accepted polarization of 92% is achieved.

3.2.2 *Removal of positrons*

The μSR technique gives the magnetic characteristics of the sample by measuring the information of the outgoing positrons that decay when muons are stopped in the

Table 3 Component parameters of the beamline

	Length (mm)	Inner aperture (width and height) (mm)	Field at r = 20 cm	Focus direction
Q1	300	Diameter = 400	1.685 kG	Vertical
Q2	300	Diameter = 400	1.498 kG	Horizontal
Q3	300	Diameter = 400	1.276 kG	Vertical
Q4	300	Diameter = 400	1.347 kG	Horizontal
Q5	300	Diameter = 400	1.171 kG	Horizontal
Q6	300	Diameter = 400	1.148 kG	Vertical
Q7	300	Diameter = 400	1.200 kG	Horizontal
Q8	300	Diameter = 400	1.800 kG	Vertical
Q9	300	Diameter = 400	1.650 kG	Horizontal
Dipole (RB1 and RB2)	494.3	W = 500, H = 300	0.978 kG	
Wien filter	$l_{\mathrm{E}} = l_{\mathrm{B}}$ = 600	$W = H$ = 400	E = 2 MV/m B = 260 G	Horizontal deflection

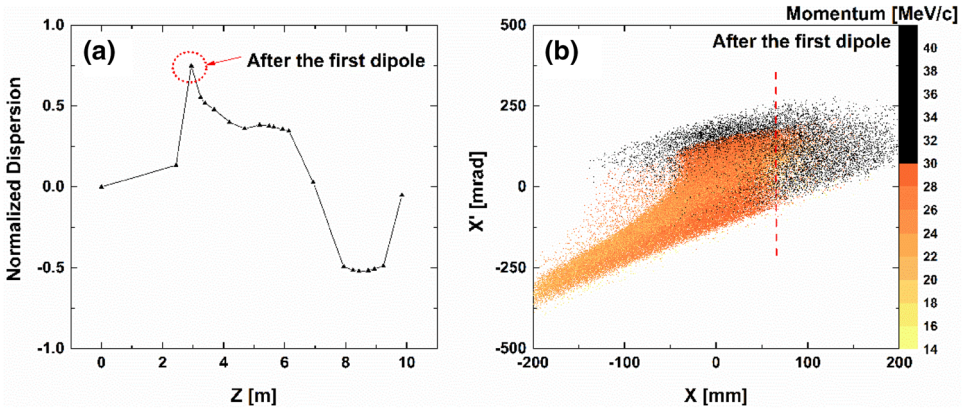

Fig. 9 **a** Normalized dispersion function along this beamline, **b** x–x' phase map of muons with different momentums at maximum normalized dispersion

material. Usually, positrons from the target are the dominant in-beam background particles for a muon source and must be minimized. In this case, we employ a Wien filter to deflect out the positrons that have the same momentum as the reference muons. Avoiding vital reduction of the muon beam polarization, the length of the Wien filter is chosen as 0.6 m. Moreover, an additional collimator (collimation for $x \leq 50$ mm) at the entrance of the down-streaming quadrupole Q7 helps to block the biased positions as shown in Fig. 10.

3.2.3 *Small beam spot at the experimental sample*

In general, given that the size of the μSR experiment sample is small, the size of the beam spot should be controlled within approximately Ø30 mm (FWHM). If no collimation is applied, the beam spot and profiles tend to be large and are given in Fig. 7. Collimation using slits is used to reduce the beam spot size. The transfer matrix between two points s_2 and s_1 in the beamline could be expressed as Eq. (4) [17],

$$M(s_2|s_1) = \begin{pmatrix} \sqrt{\frac{\beta_2}{\beta_1}}(\cos\psi + \alpha_1 \sin\psi) & \sqrt{\beta_1\beta_2}\sin\psi \\ -\frac{1+\alpha_1\alpha_2}{\sqrt{\beta_1\beta_2}}\sin\psi + \frac{\alpha_1-\alpha_2}{\sqrt{\beta_1\beta_2}}\cos\psi & \sqrt{\frac{\beta_1}{\beta_2}}(\cos\psi - \alpha_2\sin\psi) \end{pmatrix}, \tag{4}$$

where α, β are the Twiss parameters and ψ is the phase function. In addition, the transport equation between the two points is expressed as follows:

$$\begin{pmatrix} x_2 \\ x_2' \end{pmatrix} = M(s_2|s_1)\begin{pmatrix} x_1 \\ x_1' \end{pmatrix}. \tag{5}$$

Thus, x_2 and x_1 will be multiples if the element M_{12} is equal to zero. This means that $\sin\psi = 0$, that is,

$$\psi = n\pi\,(n = 0, 1, 2\ldots). \tag{6}$$

In this beamline, $\psi = \pi$ would be a good choice for collimation. Figure 11 shows the phase shift in the x-direction and y-direction for the entire beamline. For a uniform distribution, the phase shift is 180° from z = 6620 mm to the final spot in the x-direction and z = 3970 mm in the y-direction.

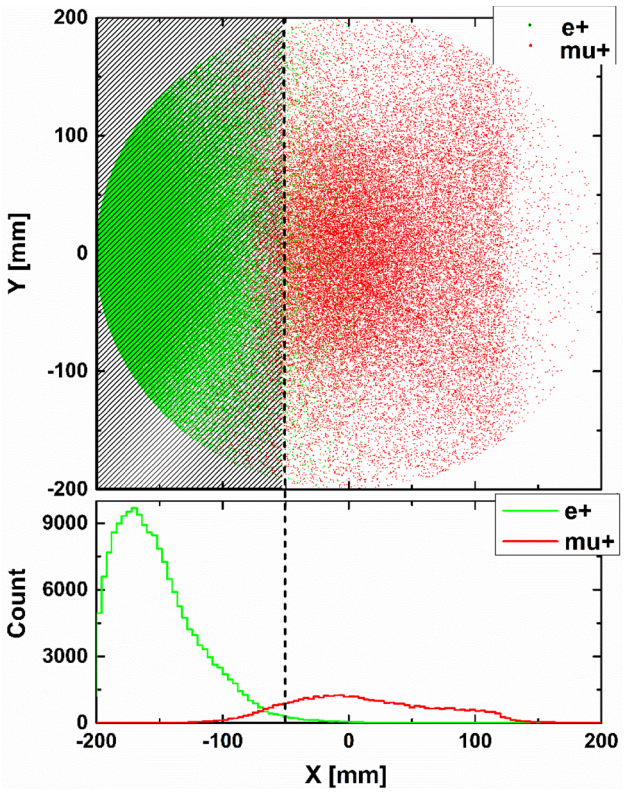

Fig. 10 Positron and muon distributions at the entrance of Q7 and the collimator (shadowed part)

Considering nonlinear effects and simulated distributions from the target, these positions will be slightly adjusted. Three groups of slits are placed at different positions along the z-axis as shown in Table 4. With collimation of three slits, beam spot and profiles are shown in Fig. 12. The shape of the beam spot is an approximate square, and the FWHM values are approximately 30 mm. The flux within the FWHM (30 mm × 30 mm) is

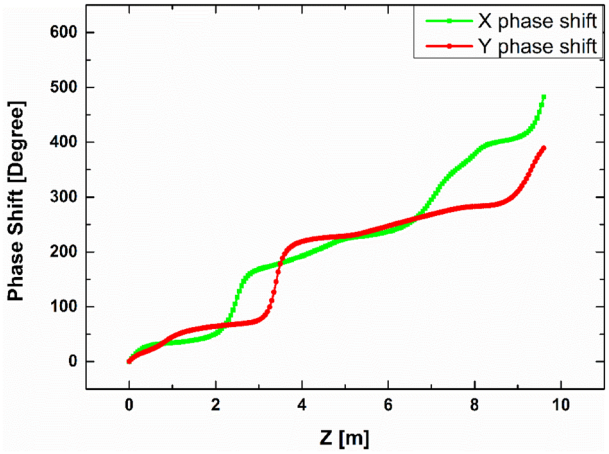

Fig. 11 Phase shift of the uniform distribution beam within the nominal acceptance

approximately 1.2 × 10^5 μ^+/s. The momentum is slightly larger than 10%.

Considering the different cases of collimation in the beamline, several backgrounds are shown in Table 5. Other particles, especially positrons, are successfully swept off. The low background meets the requirement of the μSR experiments.

4 Conclusion

A simplified EMuS muon beamline was designed by considering the use of room-temperature magnets. The collimation of a small beam spot and background control were studied in detail. The flux of positive muon was determined to be larger than 1.0E+05 μ^+/s within a small beam spot. The beam polarization with respect to the beam

Table 4 Positions and parameters of the slits

	Z position (mm)	Slit width (mm)	Collimation direction
Slit-1	3970 (in front of the second bend magnet)	50	Vertical
Slit-2	6620 (behind the Wien filter)	80	Horizontal
Slit-3	7834 (in front of the Q41)	100 (horizontal) and 60 (vertical)	Horizontal and vertical

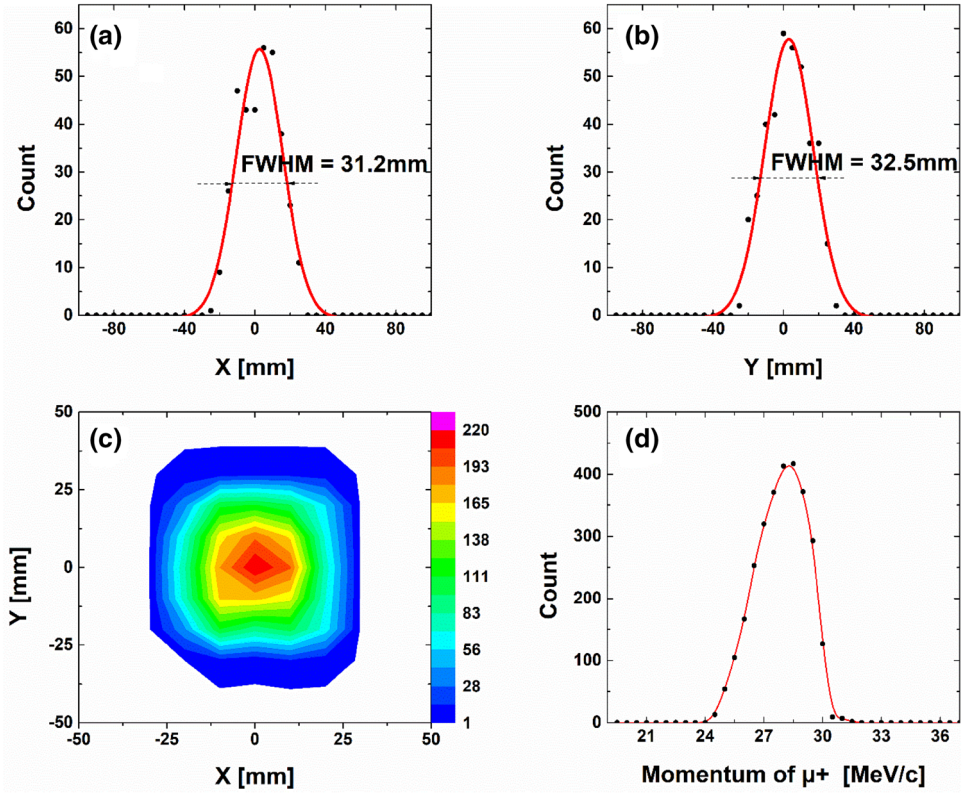

Fig. 12 Resultant beam spot and profiles with slits. **a** Profile at $y = 0$, **b** profile at $x = 0$, **c** beam spot, **d** momentum spread

Table 5 Particle composition of the beam with different cases

	Without Wien filter and collimators (%)	Wien filter + collimators (%)	Wien filter + collimators + 3 sets of slits (%)
pi+	< 0.1	< 0.1	< 0.1
mu+	~ 7	> 99	> 99
e+	> 85	< 1	Almost none
Proton and others	~ 4	Almost none	Almost none

axis was slightly better than 90%, and the contamination from other particles was less than 1%. Subsequently, a suitable engineering design will be implemented. We hope that this will be the first muon beamline built in China.

Acknowledgements The author would like to thank all colleagues in the EMuS collaborations.

References

1. F. Foroughi, E. Morenzoni, T. Prokscha et al., Upgrading the PSI muon facility. Hyperfine Interact. **138**(1–4), 483–488 (2001). https://doi.org/10.1023/A:1020830830050
2. R. Abela, F. Foroughi, D. Renker, Muon beams at PSI. Z. Phys. C Part. Fields **56**(1), S240–S242 (1992). https://doi.org/10.1007/BF02426803
3. T. Prokscha, E. Morenzoni, K. Deiters et al., The new μE4 beam at PSI: a hybrid-type large acceptance channel for the generation of a high intensity surface-muon beam. Nucl. Instrum. Methods A **595**(2), 317–331 (2008). https://doi.org/10.1016/j.nima.2008.07.081
4. G.M. Marshall, Muon beams and facilities at TRIUMF. Z. Phys. C Part. Fields **56**(1), S226–S231 (1992). https://doi.org/10.1007/BF02426801
5. J.L. Beveridge, J. Doornbos, D.M. Garner, Muon facilities at TRIUMF. Hyperfine Interact. **32**(1–4), 907–912 (1986). https://doi.org/10.1007/bf02395002
6. A.D. Hillier, D.J. Adams, P.J. Baker et al., Developments at the ISIS muon source and the concomitant benefit to the user community. J. Phys. Conf. Ser. **551**, 012067 (2014). https://doi.org/10.1088/1742-6596/551/1/012067
7. T. Matsuzaki, K. Ishida, K. Nagamine et al., The RIKEN-RAL pulsed muon facility. Nucl. Instrum. Methods A **465**, 365–383 (2001). https://doi.org/10.1016/S0168-9002(01)00694-5
8. Y. Miyake, K. Shimomura, N. Kawamura et al., J-PARC muon facility, MUSE. Phys. Proc. **30**, 46–49 (2012). https://doi.org/10.1016/j.phpro.2012.04.037
9. P. Strasser, A. Koda, et al. Status of the new surface muon beamline at J-PARC MUSE, in *Proceeding of 14th International Conference on Muon Spin Rotation, Relaxation and Resonance (μSR2017)* (2018), p. 011061. https://doi.org/10.7566/jpscp.21.011061
10. R. Kadono, Y. Miyake, MUSE, the goddess of muons, and her future. Rep. Prog. Phys. **75**(2), 026302 (2012). https://doi.org/10.1088/0034-4885/75/2/026302
11. H.S. Chen, X.L. Wang, China's first pulsed neutron source. Nat. Mater. **15**(7), 689–691 (2016). https://doi.org/10.1038/nmat4655
12. H.T. Jing, C. Meng, J.Y. Tang et al., Production target and muon collection studies for an experimental muon source at CSNS. Nucl. Instrum. Methods A **684**(684), 109–116 (2012). https://doi.org/10.1016/j.nima.2012.05.045
13. K. Nagamine, Pulsed μSR facility at the KEK Booster. Hyperfine Interact. **8**(4–6), 787–795 (1981). https://doi.org/10.1007/BF01037563
14. A. Ferrari, P. R. Sala, A. Fasso, et al. *FLUKA: A Multi-Particle Transport Code*. Technical report, CERN-2005-10 (2005). https://doi.org/10.2172/877507
15. PSI Graphic Transport Framework, by U. Rohrer based on a CERN-SLAC-FERMILAB version by K.L. Brown et al
16. T. J. Roberts, D. M. Kaplan, G4beamline simulation program for matter-dominated beam lines, in *2007 IEEE Particle Accelerator Conference (PAC)*. https://doi.org/10.1109/pac.2007.4440461
17. S.Y. Lee, *Accelerator Physics*, 3rd edn. (M. World Scientific, Singapore, 2011). https://doi.org/10.1142/8335